WPTFV-CPR(18) 19916

S Varoutis et al.

Effect of plasma screening on pumping efficiency in the DEMO divertor

Preprint of Paper to be submitted for publication in Proceeding of
30th Symposium on Fusion Technology (SOFT)

This work has been carried out within the framework of the EUROfusion Consortium and has received funding from the Euratom research and training programme 2014-2018 under grant agreement No 633053. The views and opinions expressed herein do not necessarily reflect those of the European Commission.

Effect of neutral screening on pumping efficiency in the DEMO divertor

S. Varoutis, Yu. Igitkhanov and Chr. Day

Karlsruhe Institute of Technology (KIT), Institute for Technical Physics, Karlsruhe, Germany

stylianos.varoutis@kit.edu

The neutral gas screening by plasma on the top of the private flux region of the DEMO divertor configuration without dome is analysed by using the direct simulation Monte Carlo method (DSMC). Calculations show that a strong neutral outflux from the private flux region towards the confined plasma can be supressed because the neutral pressure is balanced by the magnetized plasma in the scrape-off layer. The neutral pressure in the divertor plenum rises when interaction with the plasma is taken into account and the neutral outflux is reduced with increasing plasma density and temperature at the separatrix. However, the neutral screening effect turns out to be insufficient for increasing the pumping efficiency. To achieve this goal, a dome structure has to be introduced. The DEMO divertor dome structure can be further optimized by taking into account the neutral screening effect at the top of private flux region.

Keywords: DEMO reactor; divertor; fuelling; pumping efficiency; DSMC method; neutral modelling

1. Introduction

In existing fusion machines, dome structure is introduced in the divertor to improve the pumping efficiency, compress the neutrals in the private-flux region (PFR) and protect the main plasma from neutral outflux. However, the dome reduces the flexibility of the magnetic configuration and adds to the cost of the machine, and so there is a strong incentive to either reduce its size or even remove it completely. This is why in the European DEMO programme, a domeless divertor was taken as starting point, and a programme was started to assess the necessity to have a dome.

In our previous papers [1,2] we have shown that the complete removal of the dome would cause a strong outflux of neutrals from the PFR to the main plasma and would increase the pumping speed necessary to keep the particle throughput limits. In these calculations we ignored the fact that neutrals can be screened by the hot confined plasma from the scrape-off layer (SOL) at the separatrix area and the x-point.

In the present paper we re-estimate the effect of the dome removal on the divertor performance in DEMO by taking into account the possible screening of the neutrals escaping from the PFR towards the main plasma.

The screening of the neutrals in the PFR from a magnetically confined plasma in the SOL could occur due to the fact that the penetration depth of the neutrals depends on the ionization and the charge exchange rates and becomes about 10^{-3} and 0.1 m at the densities 10^{20} and 10^{19} m^{-3}, respectively, and the plasma temperatures about 20 eV assumed at the separatrix in DEMO under different divertor operation conditions (attached or detached operation).

The plasma from the confined region could also penetrate in the PFR due to cross field diffusion, drifts and the filament transport [3,4] and is rather moderate in plasma density. In equilibrium, the neutral density in the PFR is built up by neutralized particles coming from the divertor plates (see Fig. 1). The boundary between the neutral gas and magnetically confined plasma is formed close to the separatrix and could be rather narrow of about of the penetration length.

We consider for simplicity only deuterium molecules and atoms. They undergo ionization and dissociation due to collisions with plasma particles and recombination due to divertor wall interaction.

Below, we estimate first the effect of the plasma density and temperature at the separatrix on the outflux of D_2 and D through the separatrix $\Phi_{outflux}$ in the hot plasma and on the pumping flux to the pumping port Φ_{pump} (see Fig. 1). The particle flux Φ_{in} corresponds to the incoming neutral throughput from lower part of the separatrix from the low field (LFS) and high field side (HFS).

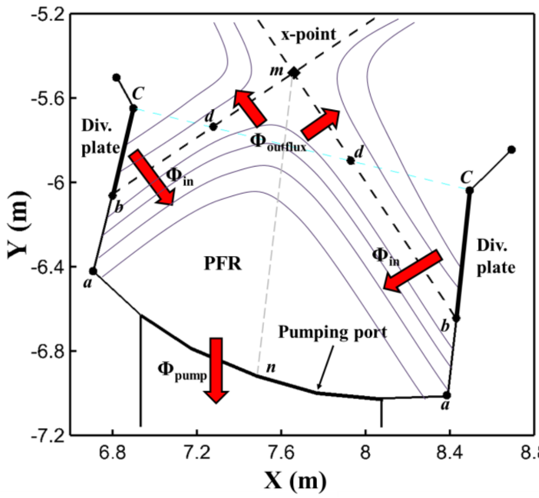

Figure 1: Sketch of DEMO divertor module as used for the numerical calculations. The area below the separatrix corresponds to the defined computational domain.

Juri.Igitkhanov@partner.kit.edu

Following that, we will define the 2D divertor model for numerical calculations, the boundary conditions and the atomic processes. Then, after short discussion of the numerical approaches, the results of calculations and the conclusions will be presented.

2. Model of DEMO divertor PFR, boundary conditions and atomic processes

In the present work, a simplified configuration of the 2015 DEMO divertor design without the dome structure is considered (see Fig. 1) [5]. In Fig. 1, a 2D cut along a poloidal plane is presented, in which the separatrix and the pumping port, are indicated. The neutral D_2 molecules enter the PFR after neutralization of plasma ions on the divertor plates. The incoming neutral flux Φ_{in}, is specified by imposing the neutral pressure P_0 and temperature T_0 on both separatrix sections *bd*. In all the present calculations they are assumed to be equal to 10 Pa and 4023 K (or 0.35 eV) respectively. The outgoing neutral fluxes $\Phi_{outflux}$ and Φ_{pump} would be an outcome of each simulation. The $\Phi_{outflux}$ takes into account the particles crossing the separatrix towards the SOL and those who are penetrating to the main plasma through the x-point vicinity. In the presence of a dome the outflux is equal to zero and the particles hitting the *dmd* section undergo diffuse reflection and are thermalized according to the wall temperature equal to T_{wall}=420 K. The plasma penetrates the PFR across the upper region of the separatrix legs (i.e. sections *dm*), on which the plasma density and temperature are specified.

The particles are removed from the PFR through the pumping port located at the bottom of the divertor cassette, on which a capture coefficient ξ (i.e $0 \le \xi \le 1.0$) is imposed. It is noted that ξ represents the imposed condition of fixed pumped particle flux and is related to the effective pumping speed S_{eff} at the pumping port with the following expression

$$S_{eff} = \frac{1}{4} A \xi v_{th}, \quad (1)$$

where A is the area of the pumping port and v_{th} is the mean thermal velocity.

In the present work the capture coefficient has been varied to take the values ξ=0.1, 0.3 and 0.6 (while low ξ values between 0.1 and 0.3 are technically achievable) [6]. If the particle is not finally absorbed from the pumping port surface, then it undergoes a diffuse reflection, assuming that the temperature at the entrance to the pump is equal to 420 K. Additionally, when molecules or atoms move across the separatrix towards the SOL, they are removed from the computational domain.

The gas-surface interaction processes considered in the PFR, is shown in Table 1, in which the surface processes and corresponding coefficients, are presented. It is assumed that the molecules which impact the wall surfaces will return into the plasma volume with a Maxwellian distribution function based on the wall temperature equal to T_{wall}=420 K. In addition, backscattered deuterium atoms when impacting the wall are recombined to deuterium molecules based on a given recombination probability equal to 0.4 [7] for the case of tungsten wall. The rest of the deuterium atoms are backscattered from the wall with the probability equal to 0.6 [7]. The plasma particles which collide with the walls are assumed to be absorbed and removed from the computational domain.

The volumetric atomic and molecular processes are presented in Table 1. The molecular deuterium dissociation and the deuterium atom ionization are considered. The corresponding rate coefficients as a function of the electron temperature in eV are provided.

Table 1: Reaction set with rate coefficients for electron collisions; The electron temperature in eV.

Reaction	Rate coefficient (m^3s^{-1})	Ref.
$D_2+e \rightarrow e+2D$	$8.4 \times 10^{-14} T^{0.45} \exp(-11.18/T)$	[8]
$D_2+e \rightarrow 2e+D+D^+$	$9.4 \times 10^{-16} T^{0.45} \exp(-29.9/T)$	[8]
$D+e \rightarrow 2e+D^+$	$9.0 \times 10^{-15} T^{0.5} \exp(-13.6/T)$	[9]
$D_2+e \rightarrow 2e+D_2^+$	$6.74 \times 10^{-14} T^{0.5} \exp(-15.72/T)$	[9]

3. Numerical approach

In this work the Direct Simulation Monte Carlo (DSMC) method has been applied, which is proven to be a reliable numerical tool to describe the behavior of rarefied gases in the divertor area. Detailed description of this method can be found in the following publications [1,10,11]. In the present work only the essential aspects of the implementation are mentioned. It is noted that the numerical code SPARTA [12] is applied in all current simulations. Briefly, the simulated number of particles ranges between 4×10^7 to 7×10^7, while the time step is equal to $\Delta t = 10^{-9}$ s. For all cases, a cartesian hierarchical grid has been implemented [12]. The total number of the computational cells is of the order of 10^6. It is noted that all the chosen values related to the number of simulated particles, the time step Δt and the size of the computational grid, have been chosen so as to ensure a standard deviation of less than 5% in the results. Each simulation needs several days for reaching steady state conditions by using an HPC and in particular 128 CPUs for each run. For all simulated cases the particle balance of the total incoming and outgoing particles in the flow domain is satisfied.

4. Results and discussion

In Fig. 2 and 3, contours of molecular deuterium number density and pressure as well as streamlines are presented, for various plasma densities and temperatures at the separatrix. It is clearly seen that by increasing plasma density and temperature, the neutral density and pressure drop at the upper part of the PFR. Additionally, the plasma affects the flow pattern of neutrals by significantly reducing the outflux of neutrals through the separatrix. The same effect is demonstrated on the profiles of deuterium density and pressure along the line segment *mn* (see Fig. 1), connecting the x-point and the

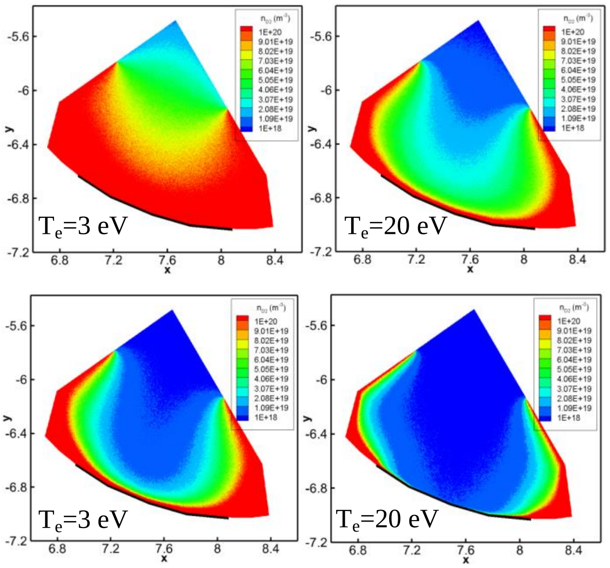

Figure 2: Contours of molecular deuterium number density for plasma density 10^{19} m^{-3} (upper) and 10^{20} m^{-3} (bottom), two plasma temperatures at the separatrix and ξ=0.3.

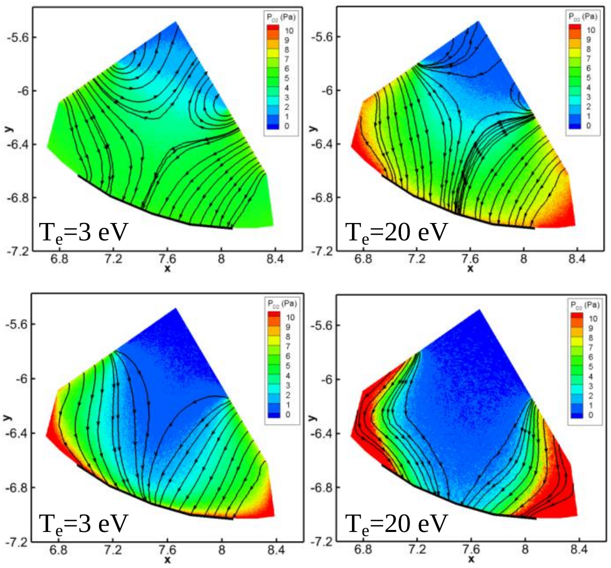

Figure 3: Contours of molecular deuterium pressure and streamlines for plasma density 10^{19} m^{-3} (upper) and 10^{20} m^{-3} (bottom), various plasma temperatures at the separatrix and ξ=0.3.

middle of the pumping port (see Fig. 4). Despite of the statistical noise in the Monte Carlo method, the clear dependence of neutral density and pressure on the plasma parameters at the separatrix is seen. This effect is more pronounced in the vicinity of the x-point, where the electrons are mainly interacting with neutrals rather than near the pumping port.

In Fig. 5a and 5b the normalized outflux of molecular and atomic deuterium through the separatrix depending on electron temperature and capture coefficient ξ for various plasma densities is shown. The molecular outflux in general decreases with the plasma density and temperature increase (compared with the case without plasma, represented in Fig. 5a by black solid line). For $n_e=10^{19}$ m^{-3} an order of magnitude drop is found in the considered temperature range. For low plasma density $n_e=10^{18}$ m^{-3} a weak dependence on plasma temperature is observed. For higher densities, namely $n_e=10^{20}$ m^{-3}, the outflux is negligible compared with the incoming neutral particle flux Φ_{in}. For the case of atomic deuterium, the outflux is considerably lower than the molecular one and in general its behavior appears to be more complicated, due to the competition between volumetric dissociation and ionization processes. This behavior is more pronounced for the case of plasma density $n_e=10^{19}$ m^{-3}, in which a roll-over is clearly seen.

In Fig. 5c, the comparison of the molecular outflux depending on the capture coefficient ξ for various plasma densities and temperatures shows the same behavior, namely the outflux decreases with increasing both the plasma parameters and the capture coefficient ξ. The neutral screening effect can be assessed from a direct comparison between the upper curve, which corresponds to the case without plasma and the rest of the curves, corresponding to various plasma parameters. In particular, the neutral outflux for ξ=0.3 and plasma density 10^{19} m^{-3}, decreases about ~87% for plasma temperature 20 eV and about ~15% for plasma temperature 3 eV compared with the case without plasma (black solid line).

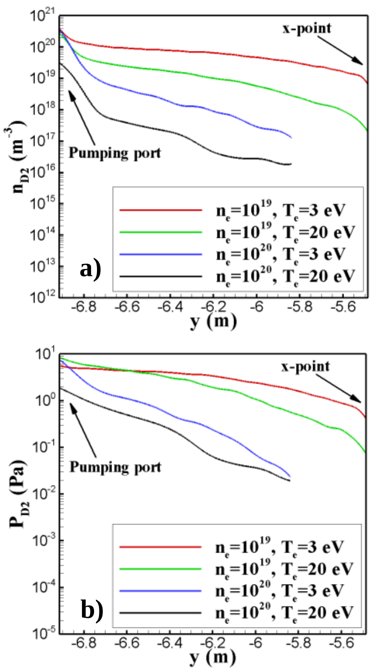

Figure 4: Distribution of molecular deuterium (a) number density and (b) pressure along the line segment *nm* (see Fig. 1), for various plasma densities and temperatures at the separatrix and ξ=0.3.

In Fig. 6a, the pumped flux through the pumping port normalized with the total incoming to PFR particle flux (so called pumping efficiency) is depicted in terms of the separatrix plasma temperature and density. Unlike the neutral outflux, the pumping efficiency increases by increasing plasma parameters, although this dependence is less pronounced for both plasma density and temperature. The reason for this behaviour is the low Knudsen number met during the DEMO divertor operational conditions (Kn~10^{-2}). More specific, due to the high collisionality in the PFR, the flow conditions close to the entrance of the pumping port are almost independent from the upstream flow conditions close to the separatrix. Similar trend was observed in a recent work considering the 3D DEMO divertor configuration with and without the dome structure [6]. The weak dependence of the pumping efficiency on the plasma parameters is also seen in Fig. 6b, where the pumping efficiency is shown in terms of the capture coefficient ξ for various plasma parameters. The upper and lower curves correspond to the case with and without the dome respectively and no plasma effects. The pumping efficiency in the presence of plasma lies between those two limit cases indicating that the neutral screening effect cannot provide the same level of pumping efficiency as in case with the dome structure.

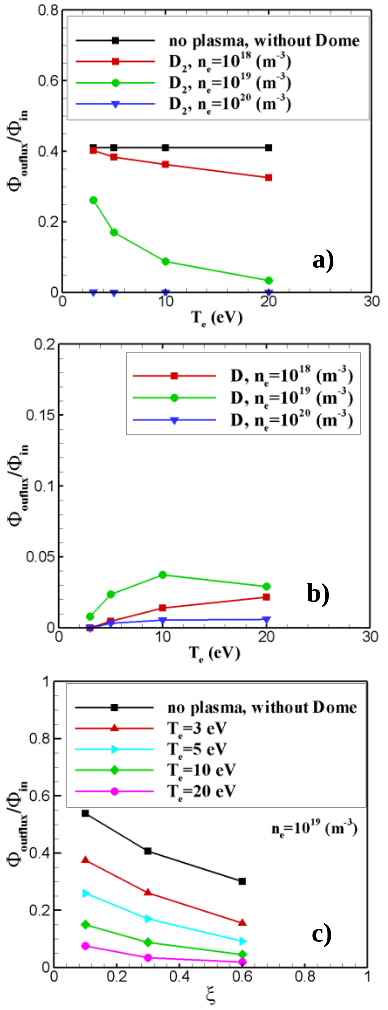

Figure 5: (a) Outflux of molecular deuterium and (b) Outflux of atomic deuterium, through the separatrix versus plasma temperature, for various plasma densities and ξ=0.3. (c) Outflux dependence on the capture coefficient ξ and various plasma temperatures.

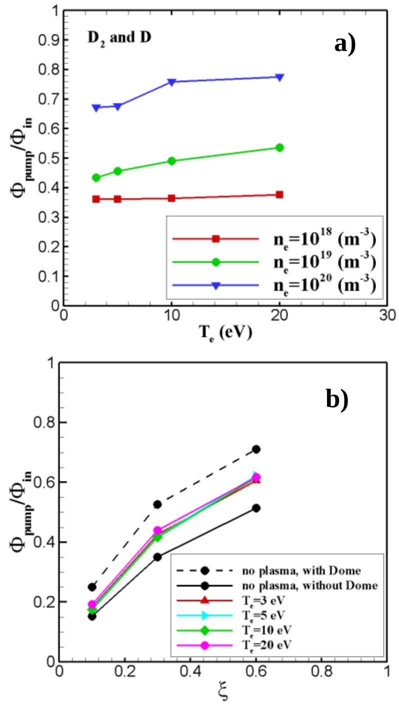

Figure 6: Normalized pumped flux of neutrals (i.e. both molecular and atomic deuterium) through the pumping port versus (a) plasma temperature and various plasma densities and (b) capture coefficient ξ for plasma density 10^{19} m^{-3}.

5. Conclusions

The screening of a neutral gas from the SOL plasma at the top of the private flux region of the DEMO divertor configuration without the dome structure is analysed. The effect of the neutral gas behaviour in the PFR is assessed by using the direct simulation Monte Carlo method for the modelling of neutral molecule dissociation and ionization as a result of collisions with plasma electrons.

It is shown that by increasing plasma density and temperature at the separatrix, the neutral density and pressure drop at the upper part of the PFR, which is bounded with magnetically confined plasma. Additionally, the plasma affects the flow pattern of neutrals by significantly reducing the outflux of neutrals through the separatrix.

For the molecular gas outflux, it is seen that for low plasma density at the separatrix a weak dependence on plasma temperature is observed, whereas for higher plasma densities the outflux is considerably reduced becoming negligible compared with the incoming neutral particles.

The neutral screening effect, namely the reduction of the outflux, may be quantified in the range of 87% at higher plasma temperatures and 15% at low plasma temperatures, for the case of ξ=0.3 and the expecting plasma densities at the separatrix (depending on attached or detached operation cases).

Regarding to pumping efficiency, the small Knudsen number expected in the DEMO divertor makes the dependence of the pumped flux on plasma parameters at the separatrix rather weak.

Concluding, it can be stated that when the neutral screening effect is taken into account, it substantially reduces the outflux of neutrals towards the x-point however the pumping efficiency is weakly improved.

The present calculations show that the plasma screening effect should be taken into account in the DEMO divertor dome design optimization.

Acknowledgments

This work has been carried out within the framework of the EUROfusion Consortium and has received funding from the Euratom research and training programme 2014-2018 under grant agreement No 633053. The views and opinions expressed herein do not necessarily reflect those of the European Commission. This work was performed within the 2nd cycle of MARCONI-FUSION HPC. The required computational resources were allocated under the project DIVGAS-KIT.

References

[1] Chr. Day, S. Varoutis and Yu. Igitkhanov, "Effect of the dome on the collisional neutral gas flow in the DEMO divertor", IEEE Trans. Plasma Sc., vol. 44(9), pp. 1636–1641, 2016.

[2] S. Varoutis et al., "Optimization of pumping efficiency and divertor operation in DEMO", Nucl. Materials and Energy, vol. 12, pp. 668-673, 2017.

[3] B. Lehnert, "Screening of a high-density plasma from neutral gas penetration", Nucl. Fusion, vol. 8 (3), pp. 173-181, 1968.

[4] J.R. Harrison, G.M. Fishpool, B.D. Dudson, "Filamentary Transport in the Private Flux Region in MAST", J. Nucl. Mater., vol. 463, pp. 757–760, 2015.

[5] R. Wenninger et al., "The physics and technology basis entering European system code studies for DEMO", Nucl. Fus., vol. 57, pp. 016011, 2017.

[6] S. Varoutis et al., "Effect of neutral leaks on pumping efficiency in 3D DEMO divertor configuration", FED, doi:10.1016/j.fusengdes.2018.04.089, 2018.

[7] Eirene database, http://www.eirene.de/html/surface_data.html.

[8] J.-S. Yoon, M.-Y. Song, J.-M. Han, S. H. Hwang, W.-S. Chang, B. Lee and Y. Itikawa, "Cross sections for electron collisions with hydrogen molecules", J. Phys. Chem. Ref. Data, vol. 37, pp. 913–931, 2008.

[9] J.D. Huba, "NRL Plasma Formulary", page 55, 2016, https://www.nrl.navy.mil/ppd/content/nrl-plasma-formulary.

[10] G.A. Bird, "*Molecular Gas Dynamics and the Direct Simulation of Gas Flows*", Oxford University Press, Oxford, UK, 1994.

[11] S. Varoutis et al., "Simulation of neutral gas flow in the JET sub-divertor", FED, vol. 121, pp. 13–21, 2017.

[12] M. Gallis, et al., "Direct simulation Monte Carlo: the quest for speed", in: AIP Conf. Proc., vol. 1628, 2014.